

# The effect of cluster formation on mass separation in binary molecular beams

Wei Li,<sup>a)</sup> M. J. Stirniman,<sup>b)</sup> and S. J. Sibener<sup>c)</sup>

*The James Franck Institute and Department of Chemistry, The University of Chicago, Chicago, Illinois 60637*

(Received 15 July 1999; accepted 17 November 1999)

The downstream composition of a skimmed supersonic binary molecular beam originally consisting of a 20% neon/80% xenon mixture before expansion has been studied as a function of nozzle stagnation pressure. We have found that the neon to xenon ratio dropped dramatically as the stagnation pressure was increased at low nozzle temperature (303 K), a drop which cannot be well described by existing theory. Time-of-flight (TOF) measurements indicate that Xe clustering occurs as the stagnation pressure is increased. This clustering coincides with the additional Ne depletion we observe. At a higher nozzle temperature where Xe clustering does not occur (573 K), this measured mass separation phenomenon is absent. Similar experiments have been done for another binary mixture, 20% O<sub>2</sub>/80% Xe. Similar anomalous mass separation is observed with this mixture, confirming the attribution of this phenomenon to clustering of the more massive component of the mixture. These findings have implications for novel methods of gas-dynamics-based mass separation potentially including isotope enrichment. © 2000 American Institute of Physics. [S0021-9606(00)01806-7]

## I. INTRODUCTION

Supersonic molecular beam techniques are widely used in the study of gas-phase and gas-surface collision phenomena. In many applications, one uses mixed, i.e., seeded, beams to accelerate or decelerate a species in order to tune its energy over a rather wide range.<sup>1,2</sup> It has been well documented that a variety of factors contribute to mass separation in such skimmed and seeded beams, which can lead to substantial differences between the starting composition of the expansion gas and the characteristics of the downstream “sampled” beam.<sup>3–6</sup> This composition distortion becomes of crucial concern whenever a quantitative measurement is needed. Much effort has been made to understand and quantify such mass separation phenomena which arise during expansion.<sup>3–6</sup> Unfortunately, some confusion still exists due to the complexity of the problem, as well as the variation of measurement configurations used in these studies.<sup>7,8</sup>

In this paper, we have examined the composition changes which arise for an “antiseeded” binary mixture, in which the minority species is lighter than the carrier gas. In particular, we have examined the downstream depletion of the seed gas as a function of stagnation pressure and nozzle temperature. Neon/xenon and oxygen/xenon mixtures were used in these studies. Strong evidence is herein reported which implicates cluster formation in the heavier carrier gas as inducing downstream seed gas depletion which exceeds the levels commonly seen. Existing theories of mass separation in binary supersonic flows do not adequately account for this striking phenomenon.

## II. EXPERIMENT

The experiments were carried out in a two level ultra-high vacuum (UHV) chamber, coupled to a triply differentially pumped molecular beam line (Fig. 1), which has been described previously.<sup>9,10</sup> Briefly, the upper level of the UHV chamber contains an Auger spectrometer equipped with a double-pass cylindrical mirror analyzer, low energy electron diffraction (LEED) optics, and a sputter ion gun. The lower level contains a high resolution electron energy loss spectrometer (HREELS, model LK 2000), and a mass spectrometer (Balzers, model QMA112) situated in line-of-sight with the molecular beam from the threefold differentially pumped supersonic molecular beam source. The UHV chamber is pumped by a 300  $\ell$  s<sup>-1</sup> ion pump, a liquid nitrogen cooled titanium sublimation pump, and a 60  $\ell$  s<sup>-1</sup> turbomolecular pump, and has a base pressure of less than  $5 \times 10^{-11}$  Torr.

The molecular beam line consists of three stages. The source chamber contains a laser drilled 50  $\mu$  diam nozzle (EAM Optics) and a 0.5 mm diam Gentry (Beam Dynamics) skimmer, and is evacuated by a 10 in. diffusion pump. The second differential stage of the beamline, pumped by a 4 in. diffusion pump, contains a mechanical chopper with two 0.5 mm slits for time-of-flight (TOF) measurements and a 50% duty cycle square wave pattern which was used for phase sensitive detection. The flight path from the chopper to the center of the mass spectrometer ionizer is  $1.16 \pm 0.01$  m. The third differential stage, pumped by a 100  $\ell$  s<sup>-1</sup> turbomolecular pump, further reduces the sequential effusion from the source chamber before coupling to the UHV chamber.

The two component mixtures had initial xenon to neon or xenon to oxygen ratios of 4:1. Two detection methods were used for the measurement of the composition ratios of these binary molecular beams. Lock-in detection using the

<sup>a)</sup>Present address: Lucent/Bell Laboratories, Naperville, Illinois.

<sup>b)</sup>Present address: Seagate Technology, Fremont, California.

<sup>c)</sup>Author to whom correspondence should be addressed. Electronic mail: s-sibener@uchicago.edu

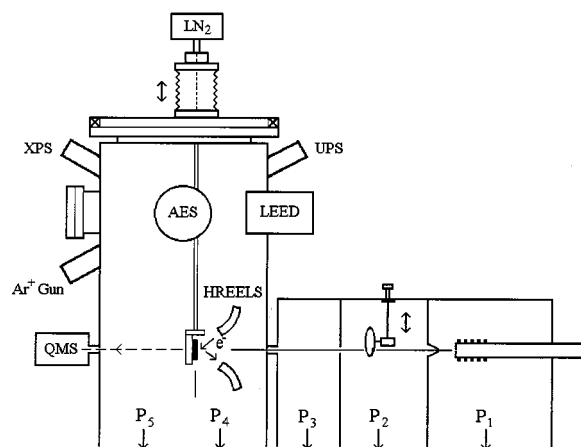


FIG. 1. Schematic side-view of the mass spectrometer containing UHV chamber coupled with the triply-differentially pumped supersonic molecular beamline. Chamber 2 of the beamline contains the multipatterned rotating disk copper used for time-of-flight modulation.

optically detected signal from the rotating chopper as the reference signal was done with the beam directed directly into the mass spectrometer ionizer. This modulated beam procedure was chosen to eliminate possible variations in background intensities due to different pumping speeds of the two components. In addition, component ratios were also detected by monitoring the background intensities in the UHV chamber with the beam intentionally colliding with a metal beam stop *before* ionization; this latter procedure was

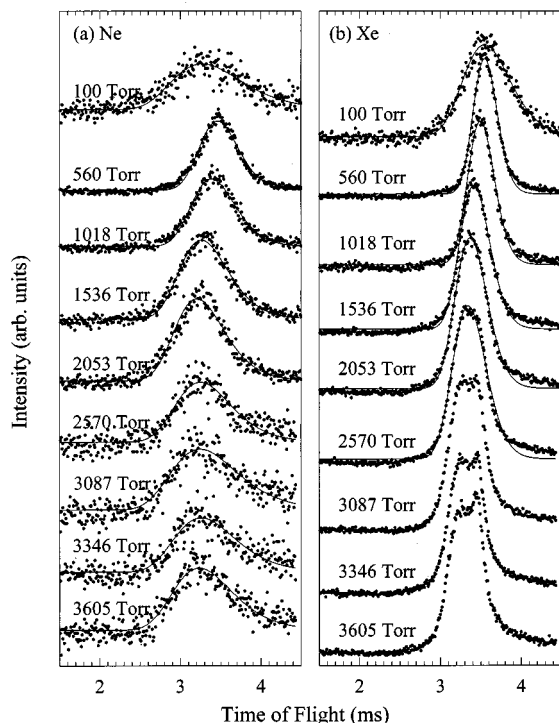


FIG. 2. TOF beam profiles for 20% Ne/80% Xe binary gas mixtures as a function of nozzle stagnation pressure with a nozzle temperature of 303 K. Solid lines are fits to the data using Eq. (2): (a) Ne component; (b) Xe component. The bimodal Xe profiles at higher pressures are indicative of cluster formation.

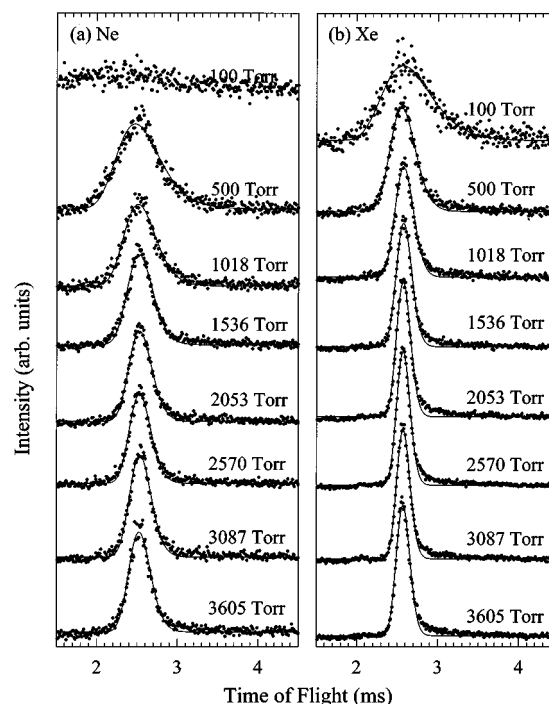


FIG. 3. TOF beam profiles for 20% Ne/80% Xe binary gas mixtures as a function of nozzle stagnation pressure with a nozzle temperature of 573 K. Solid lines are fits to the data using Eq. (2): (a) Ne component; (b) Xe component. In contrast to the lower nozzle temperature data of Fig. 1, note here the absence of bimodality in the higher pressure Xe profiles.

introduced to eliminate any systematic detection biases during ionization due to cluster formation (i.e., surface collisions serve to break up clusters in the incident beam prior to detection). Calibration of the initial mixture was accomplished by direct admission of the mixture gas to the UHV chamber at pressures sufficient to give comparable signals to those obtained with the line-of-sight beam. The concentration of xenon was monitored using the  $m/e$  peak at 131 amu, and the neon concentration by the peak at 20 amu. TOF measurements were done using an Ortec multichannel scaler to detect the amplified and discriminated signal from the mass spectrometer in pulse counting mode. A skimmer-to-nozzle distance of 7.7 mm was used in the current study. Closer distances resulted in beam attenuation, while at larger distances a marked flight time difference between xenon and neon was observed, an indication of velocity slip between the two components.

### III. RESULTS

A series of TOF profiles of the neon and xenon components of the binary molecular beam as a function of stagnation pressure and nozzle temperature are shown in Figs. 2 and 3. Inspection of these data reveal some general trends. At the higher nozzle temperature (Fig. 3) the TOF peaks show the expected behavior, i.e., a decreasing peak width with an increase in stagnation pressure. However, for the molecular beam formed from the nozzle held at 303 K, it was observed that the TOF peak width of the neon component first decreased, and then increased [Fig. 2(a)]. Also, the TOF peak

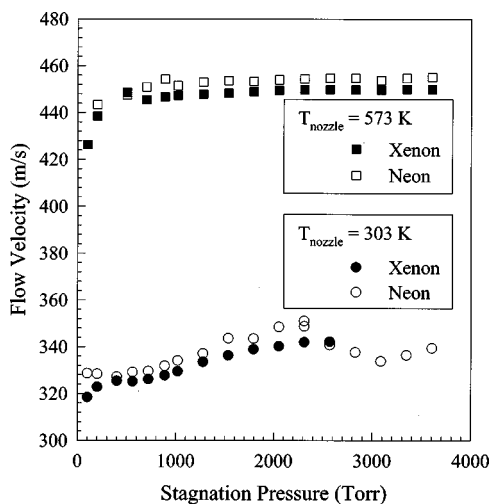


FIG. 4. Ne and Xe flow velocities calculated using Eq. (2) vs stagnation pressure for relatively low (303 K) and high (573 K) nozzle temperatures.

for the xenon component begins to show a bimodal flight time distribution for stagnation pressures above  $\approx 3000$  Torr [Fig. 2(b)].

A more detailed analysis of the TOF data was done with a velocity distribution widely used to characterize molecular beams,

$$f(v) \sim v^3 \cdot e^{-[m(v-v_0)^2]/2kT}, \quad (1)$$

where  $k$  is Boltzmann's constant,  $m$  is the molecular mass of either the neon or xenon atoms,  $v_0$  is beam flow velocity, and  $T$  is the beam temperature. Equation (1) was transformed into a function of flight time, using the Jacobian,<sup>6,11</sup>  $dv = -(L/t^2)dt$ , and corrected for the fact that we used a density sensitive detector,<sup>11</sup> to yield Eq. (2),

$$f(t) \sim \frac{L^3}{t^4} \cdot e^{-\{m[(L/t)-v_0]^2\}/2kT}. \quad (2)$$

We found that Eq. (2) afforded a good fit to the experimental TOF data, as shown by solid lines in Figs. 2 and 3. These fits allowed us to extract two parameters characteristic of our beams, the beam flow velocity  $v_0$  and the beam temperature  $T$ . Figure 4 shows the extracted beam temperatures as a function of nozzle stagnation pressure for both neon and xenon at nozzle temperatures of 573 K and 303 K. At a nozzle temperature of 573 K, the flow velocity shows expected behavior for both neon and xenon. There is an initial increase in the flow velocity as the stagnation pressure is increased, indicating the onset of a supersonic expansion, followed by a region of nearly constant flow velocity. However, different results were obtained for the beam expanded from the nozzle held at 303 K. For the neon component, we again observed an initial increase in the flow velocity with increasing stagnation pressure, but the flow velocity then decreased as the stagnation pressure was further increased. For the xenon component, Eq. (2) could be used to extract the flow velocity only up to a stagnation pressure of 2570 Torr, due to the appearance of the bimodal TOF distribution above this point.

Figure 5 shows the beam temperatures extracted from the TOF analysis as a function of stagnation pressure for the

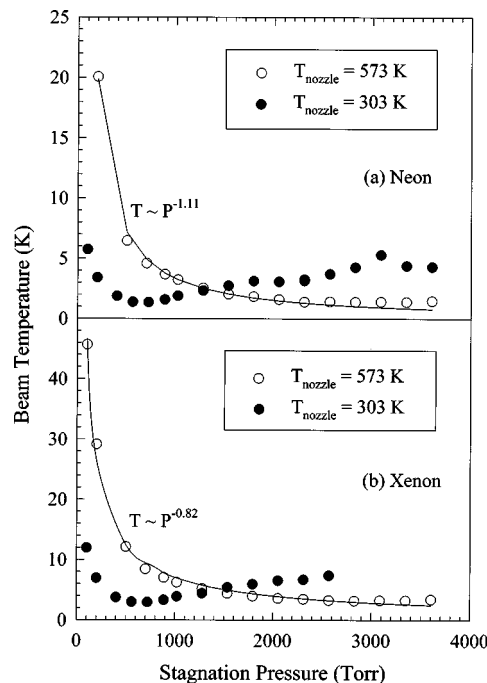


FIG. 5. (a) Terminal beam expansion temperatures calculated using Eq. (2) as a function of nozzle stagnation pressure for the Ne component of the mixture with nozzle temperatures of 303 K and 573 K. (b) Same as (a) but for the Xe component of the mixture.

two different nozzle temperatures. At a nozzle temperature of 573 K, we see a monotonically decreasing beam temperature as a function of stagnation pressure for both components, as expected for an increasingly supersonic expansion. It has been shown that the temperature of a supersonic expansion can be well described by the simple relationship

$$T \propto P^{-a}, \quad (3)$$

where  $P$  is the stagnation pressure and  $a$  is a constant close to one.<sup>12</sup> Equation (3) was used to fit the data for expansions at 573 K in Fig. 5, and good fits were obtained with  $a = 1.11$  and 0.82 for the neon and xenon components, respectively (solid lines). However, at a nozzle temperature of 303 K, the extracted beam temperature as a function of stagnation pressure first decreases, then goes through a minimum before starting to increase again. This anomalous behavior corresponds to the decrease in beam velocity observed for higher stagnation pressures at a nozzle temperature of 303 K. We would like to note that, due to the appearance of double peaks in the TOF distribution of the xenon component at 303 K nozzle temperature, the fitted beam temperature should be considered only as a parameter describing the expansion quality, and not a true measure of the beam temperature.

In Fig. 6, we have plotted the measured beam intensities for the two beam components as a function of stagnation pressure for nozzle temperatures of 573 K and 303 K. These data were taken using the modulated beam and lock-in detection method described in the experimental section. This figure again demonstrates that there is a substantial difference in the behavior of the beam for the two different nozzle temperatures. At 573 K, the intensity of both the xenon and neon components increases almost linearly as the stagnation

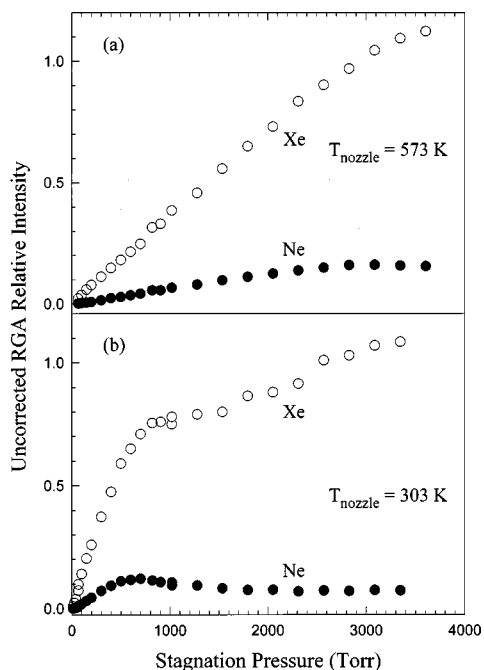


FIG. 6. Downstream Ne and Xe intensities vs stagnation pressure, using the lock-in detection method. (a) Nozzle at 573 K. These data increase essentially in a linear manner with increasing pressure, as expected for a nonclustering expansion. (b) Nozzle at 303 K. These data deviate from ideal behavior near 700 Torr due to cluster formation.

pressure is increased. (At stagnation pressures of  $\approx 3000$  Torr and above, the intensity of the molecular beam is attenuated due to the finite pumping speed of our source chamber, which results in decreased mean-free flight path and scattering of the beam components.) With the nozzle temperature held at 303 K [Fig. 6 (b)], however, we observe a maximum in the intensity of the neon component at about 700 Torr stagnation pressure. Also, the intensity of the xenon component vs stagnation pressure exhibits a sharp change in slope in the region where neon intensity begins to decrease. Somewhat more informative is the measured neon to xenon ratio in the beam as a function of the stagnation pressure for the two nozzle temperatures, which was calibrated against the intensities as measured with direct admission of the mixture gas to the UHV chamber (Fig. 7). At both nozzle temperatures, there is an initial decrease in the ratio of neon to xenon at low stagnation pressures (0–300 Torr). This effect has been ascribed to pressure gradients in the rapidly expanding gas jet in the stagnation pressure region before free molecular flow is achieved.<sup>4,12,13</sup> This so-called diffusive separation results in a concentration of the heavier species near the center line of the beam. Following this region there is an increase in the ratio of neon to xenon up to a stagnation pressure of about 700 Torr. At 573 K nozzle temperature, the component ratio levels off at this point, until stagnation pressures in the region of 3000 Torr are reached, at which point the component ratio again begins to drop. At a nozzle temperature of 303 K, however, the component ratio goes through a well defined maximum in this region, followed by a sharp decrease in the ratio of neon to xenon. To rule out experimental artifacts due to the phase sensitive detection method employed, the measurement of the beam component

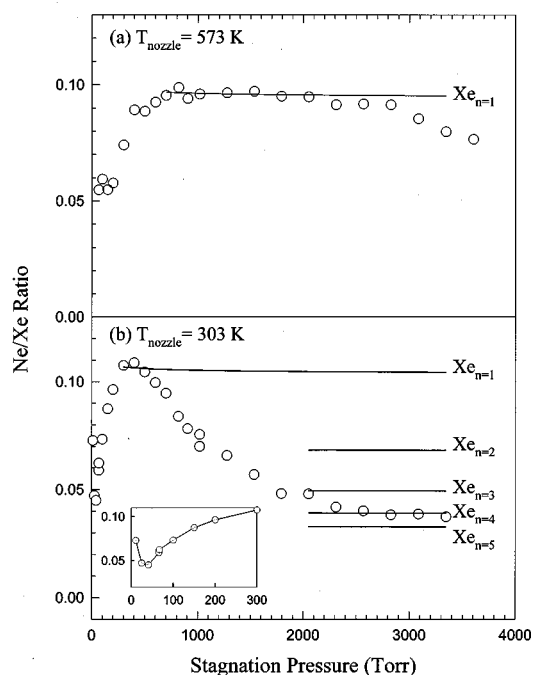


FIG. 7. Downstream Ne/Xe composition ratios (data corrected for differences in detectivity using a calibrated gas leak into the UHV chamber which had the identical composition as the beam gas cylinder, i.e., Xe:Ne ratio of 4:1) vs stagnation pressure. Data taken using lock-in detection of the chopped (modulated) beam. (a) Nozzle at 573 K; good agreement with extant theory [solid line calculated using Eq. (4) for Xe monomers]. (b) Nozzle at 303 K; marked depletion of Ne and disagreement with theory (solid line calculated as above with  $n=1$ ) after the onset of  $Xe_n$  cluster formation. Solid lines marked as  $Xe_n$  ( $n=2-5$ ) give calculated depletions assuming pure beams of each cluster size (see text). Inset shows details of the data in the low pressure regime.

intensity vs stagnation pressure was repeated using a second procedure based on measuring background intensities as described in the experimental section (i.e., clusters broken up by surface collisions prior to mass spectrometric detection of the seed and carrier gas intensities; this method is similar to the “stagnation detection mode” of Ref. 14). These data are plotted in Fig. 8, and although the absolute intensities are uncalibrated, they show that this detection method yields trends similar to those shown in Fig. 6.

#### IV. DISCUSSION

The neon to xenon ratios plotted in Fig. 7 show a marked depletion of neon in our binary molecular beam relative to the starting ratio of 0.20, especially in the case of expansion from the room temperature nozzle. Even at a stagnation pressure of 50 Torr, the lowest pressure where we could obtain a reliable signal, the neon to xenon ratio near the beam centerline is significantly different than that of the starting mixture. As mentioned earlier, the initial drop in the neon to xenon ratio can be attributed to diffusive separation, an effect which disappears as the beam becomes supersonic. For supersonic molecular beams, several authors have reported the separation effect of Mach number focusing. Mach number focusing causes depletion of the lighter species along the centerline of the beam due to the fact that the lighter components have higher velocities perpendicular to the beam direction than the

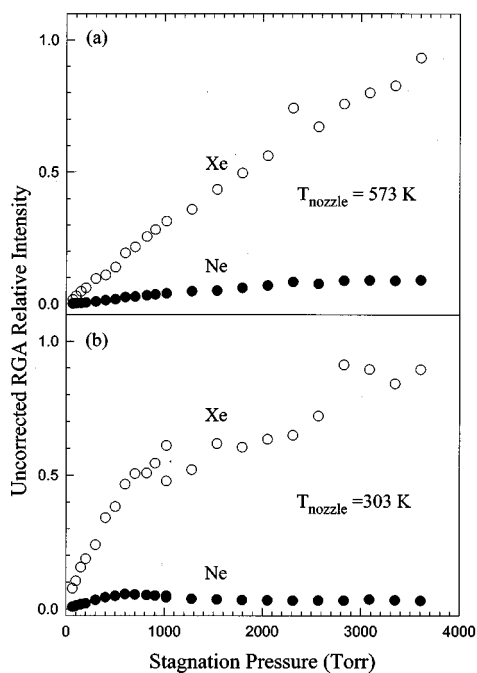


FIG. 8. Ne and Xe intensities vs stagnation pressure, using the background detection method (see text) which breaks up clusters in the incident beam via collisional dissociation prior to mass spectrometric detection of component intensities. (a) Nozzle at 573 K; (b) nozzle at 303 K.

heavier components.<sup>6,12</sup> An expression is derived in Ref. 6 for determination of the extent of this depletion,

$$\frac{n(\text{Ne})_1}{n(\text{Xe})_1} = \frac{n(\text{Ne})_0}{n(\text{Xe})_0} \cdot \frac{1 - \exp(-S(\text{Ne})_{\perp 1}^2 \xi_{\text{max}}^2)}{1 - \exp(-S(\text{Xe})_{\perp 1}^2 \xi_{\text{max}}^2)}, \quad (4)$$

where  $n$  is the number density,  $S_{\perp}$  is the hydrodynamic speed divided by the most-probable random speed perpendicular to the hydrodynamic velocity,  $\xi_{\text{max}}$  is the angle between the beam centerline and the line from the source nozzle to the skimmer lip, and the subscripts 0 and 1 refer to conditions at the source and the detector, respectively.  $S(\text{Xe})_{\perp}$  is given in Eq. (17) of Ref. 6, and  $S(\text{Ne})_{\perp}$  is related to  $S(\text{Xe})_{\perp}$ , with Eq. (21) of Ref. 6. Using the above equation, we carried out a simple calculation with known parameters, plus assuming the effective collision diameters for collision between xenon atoms as being 4.3 Å, and for collision between xenon and neon atoms as being 3.5 Å.<sup>12</sup> The solid lines in Figs. 7(a) and 7(b) with  $n=1$ , where  $n$  is the number of Xe atoms in the  $\text{Xe}_n$  cluster, are the results of this calculation. For the expansion from the nozzle at 573 K, the scaled calculation agrees with the data reasonably well in the region of 1000–3000 Torr stagnation pressure. However, in the case of expansion from the nozzle at 303 K, the scaled calculation agrees with the data only at the maximum of the neon to xenon ratio at about 700 Torr stagnation pressure. The depletion of the neon component above this stagnation pressure is much greater than that predicted by Mach number focusing with  $n=1$  alone. We have done further calculations to demonstrate that the presence of relatively small Xe clusters can account for this discrepancy. The calculated lines labeled  $\text{Xe}_n$  with  $n=2,3,4,5$  in Fig. 7(b) show the expected effect for pure beams of these cluster sizes, i.e., for beams consisting

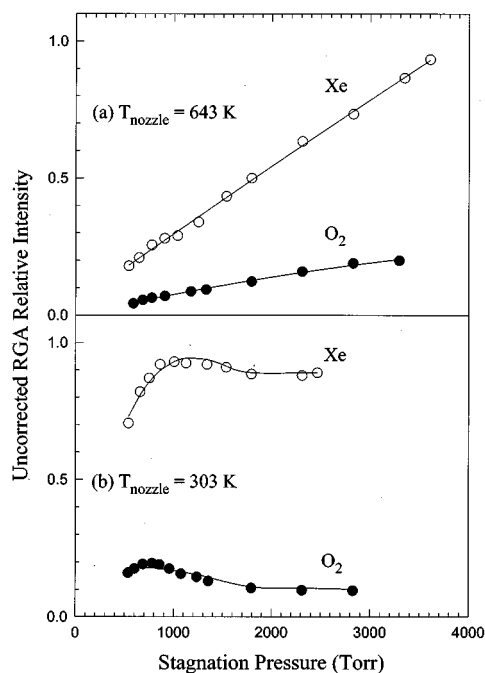


FIG. 9. O<sub>2</sub> and Xe intensities vs stagnation pressure, obtained using lock-in detection of the modulated beam. (a) Nozzle at 643 K; (b) nozzle at 303 K. Solid lines included for clarity are polynomial fits to the data.

of only a specific value of  $n$ . The effective collision diameters of the Xe clusters were calculated assuming closest-packed geometries of the clusters,  $d=(2, 2.16, 2.23, \text{ or } 2.29) \times 4.3 \text{ \AA}$  for  $n=2,3,4,5$ , respectively. A trend is seen, with clusters of systematically larger  $n$  leading to monotonically larger depletions of Ne. From this we conclude that a weighted average of these depletion factors, which properly accounted for the continuously changing  $\text{Xe}_n$  composition of the beam as a function of stagnation pressure, would clearly be capable of quantitatively fitting the pressure dependent depletion data of Fig. 7(b). This strongly supports the main finding of this paper, namely, that the unexpectedly large light-species depletion is due to the onset of cluster formation.

We recall that we have observed anomalies in parameters extracted from the beam TOF profiles for the room temperature expansion, in particular the flow velocities of the components and the temperature of the beam (Figs. 4 and 5). These anomalies begin to be evident in the region of 500–700 Torr stagnation pressures, and we believe these observations are a result of the onset of substantial xenon cluster formation in the room temperature expansion. This is supported by a simple calculation for our system and similar clustering effects observed in other systems.<sup>15</sup> The formation of xenon clusters at around 700 Torr would substantially change the components of the original beam and thus we attribute the dramatic mass separation above these stagnation pressures in the 303 K beam to the effect of these xenon clusters.

To test the hypothesis we carried out similar experiments using a xenon/oxygen binary molecular beam initially composed of a 4:1 xenon to oxygen ratio. Figure 9 shows that the measured component intensities as a function of stagnation pressure are very similar in this case as for the

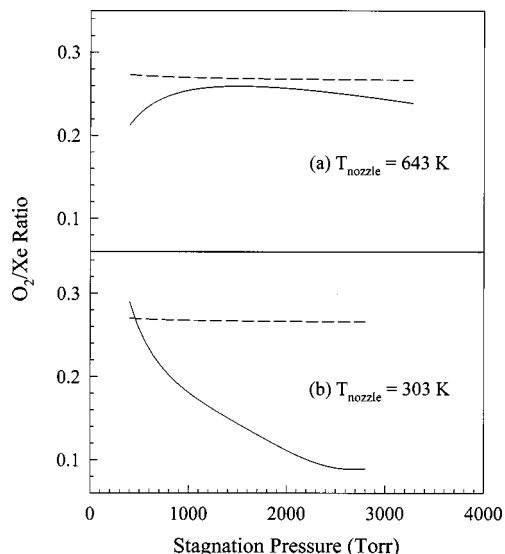


FIG. 10.  $O_2/Xe$  ratio vs stagnation pressure obtained from solid line fits of Fig. 9 with the nozzle at (a) 643 K and (b) 303 K. The dashed lines are the expected  $O_2/Xe$  ratios calculated using Eq. (4). Again note the marked deviation from theory, i.e., enhanced depletion of  $O_2$ , which occurs in the 303 K nozzle data after the onset of cluster formation.

xenon/neon molecular beam. Because measurement of the intensities of the oxygen and xenon components were not taken at the same stagnation pressure in these experiments, the data in Figs. 9(a) and 9(b) were fit with polynomial functions in order to generate plots of component ratios vs. stagnation pressure (solid lines). Figure 10 shows the oxygen to xenon ratios generated from these polynomial fits (solid lines), in comparison to the ratios calculated using Eq. (4) (dashed lines). The similarity between the behavior of the neon/xenon and oxygen/xenon binary beams is evidence that the anomalous mass separation that we observe is an effect due to the common behavior of the heavier xenon component, namely the formation of  $Xe_n$  clusters at about 700 Torr stagnation pressure.

## V. CONCLUSION

We have studied mass separation in neon/xenon and oxygen/xenon binary supersonic molecular beams. We have found that expansion of binary beams from a room temperature nozzle results in severe depletion of the lighter compo-

nent along the centerline of the beam above a certain stagnation pressure. The extent of this mass separation is not explainable by existing theories of Mach number focusing. We believe that this depletion is due to the onset of the formation of xenon clusters at these stagnation pressures. This phenomenon is robust; the precise characteristics for a given expansion will likely depend on the physical details of the nozzle/skimmer assembly used to make the measurements. Further evidence for the formation of xenon clusters is given by the anomalous behavior of the beam flow velocity and beam temperature in the same stagnation pressure region, which were extracted from beam TOF profiles. These findings have implications for novel methods of gas-dynamics-based mass separation potentially including isotope enrichment.

## ACKNOWLEDGMENTS

This work was supported by the Air Force Office of Scientific Research and, in part, by the MRSEC Program of the National Science Foundation under Award Nos. DMR-9400379 and DMR-9808595. The authors also would like to thank Professors E. L. Knuth and M. Smith for valuable discussions.

- <sup>1</sup>J. B. Anderson, R. P. Andres, and J. B. Fenn, in *Advances in Chemical Physics*, edited by J. Ross (Interscience, New York, 1966), Vol. 10, p. 275.
- <sup>2</sup>J. B. Anderson, in *Molecular Beams and Low Density Gas Dynamics*, edited by P. P. Wegener (Marcel Dekker, New York, 1974), p. 1.
- <sup>3</sup>V. Reis and J. B. Fenn, *J. Chem. Phys.* **39**, 3240 (1963).
- <sup>4</sup>F. S. Sherman, *Phys. Fluids* **8**, 773 (1965).
- <sup>5</sup>J. B. Anderson, *AICHE. J.* **13**, 1188 (1967).
- <sup>6</sup>P. K. Sharma, E. L. Knuth, and W. S. Young, *J. Chem. Phys.* **64**, 4345 (1976).
- <sup>7</sup>H. C. W. Beijerinck and N. F. Verster, *Physica C* **111**, 327 (1981).
- <sup>8</sup>T. L. Mazely, G. H. Roehrig, and M. A. Smith, *J. Chem. Phys.* **103**, 8638 (1995).
- <sup>9</sup>W. Menezes, P. Knipp, G. Tisdale, and S. J. Sibener, *Phys. Rev. B* **41**, 5648 (1990).
- <sup>10</sup>M. J. Stirniman, Wei Li, and S. J. Sibener, *J. Chem. Phys.* **103**, 451 (1995).
- <sup>11</sup>D. J. Auerbach, in *Atomic and Molecular Beam Methods*, edited by G. Scoles (Oxford University Press, New York, 1988), Vol. 1.
- <sup>12</sup>D. R. Miller, in *Atomic and Molecular Beam Methods*, edited by G. Scoles (Oxford University Press, New York, 1988), Vol. 1.
- <sup>13</sup>T. D. McCay and L. L. Price, *Phys. Fluids* **26**, 2115 (1983).
- <sup>14</sup>M. Lewerenz, B. Schilling, and J. P. Toennies, *J. Chem. Phys.* **102**, 8191 (1995).
- <sup>15</sup>E. L. Knuth, *J. Chem. Phys.* **66**, 3515 (1977).